

## Compositional dependence of the Raman frequencies and line shapes of $\text{Cd}_{1-x}\text{Zn}_x\text{Te}$ determined with films grown by molecular-beam epitaxy

D. J. Olego

*Stauffer Chemical Company, Eastern Research Center, Elmsford, New York 10523*

P. M. Raccach and J. P. Faurie

*Department of Physics, University of Illinois at Chicago, Chicago, Illinois 60680*

(Received 2 October 1985)

Raman scattering measurements are used to investigate the lattice-dynamic properties of  $\text{Cd}_{1-x}\text{Zn}_x\text{Te}$ . The samples were thin films grown by molecular-beam epitaxy on GaAs substrates. The first-order Raman spectra for the ternary samples show two sets of longitudinal- and transverse-optical (LO,TO) modes, which arise from CdTe- and ZnTe-like vibrations. The compositional dependence of the lattice frequencies is that of a typical two-mode system. The mode oscillator strengths were evaluated from the measured frequencies. The line shapes of the LO Raman bands display asymmetrical broadenings which are observed to increase with decreasing LO-TO splitting. The LO bands were fitted with the predicted line shapes of the discrete-continuum interaction and the spatial-correlation models. The Fano line-shape of the discrete-continuum interaction model allows good fittings of both sets of LO Raman bands. The spatial-correlation model does not reproduce the line shapes of the ZnTe-like LO modes for  $x \approx 0.5$ .

There is much current interest in II-VI ternary compound semiconductor for use in a variety of solid-state devices. Concomitant with the growing number of applications and the standing improvements on device performances, research efforts are being carried out in order to elucidate the intrinsic properties of the materials. The extensive investigations of  $\text{Hg}_{1-y}\text{Cd}_y\text{Te}$  are typical examples of such research activities.<sup>1</sup> This paper deals with a novel epitaxial system of II-VI binary alloys, namely  $\text{Cd}_{1-x}\text{Zn}_x\text{Te}$ . It has been recently shown that  $\text{Cd}_{1-x}\text{Zn}_x\text{Te}$  can be grown by molecular-beam epitaxy (MBE) on foreign substrates and that the epitaxial layers possess high crystalline quality.<sup>2,3</sup> Three factors have revived the attention paid to  $\text{Cd}_{1-x}\text{Zn}_x\text{Te}$ . These are (1) the possibility of MBE growth, (2) the epitaxy achieved on foreign substrate, and (3) the band-gap tunability over a large spectral range in the visible.<sup>3</sup> Nevertheless, the body of experimental knowledge of its properties is by far less developed than for other II-VI alloys. Among the few experimental investigations available, photoluminescence and EXAFS measurements have proven that the metal lattice sites are occupied randomly by the cation atoms,<sup>3,4</sup> and reflectivity measurements have pointed out a two-mode type of behavior of the lattice vibrations.<sup>5,6</sup>

We report here on the vibrational properties of  $\text{Cd}_{1-x}\text{Zn}_x\text{Te}$  determined with Raman scattering measurements. These were performed on layers grown on GaAs substrates. The Raman frequencies measured for different values of the Zn content provide an independent confirmation of the two-mode behavior of the phonon system, and are used to determine the mode oscillator strengths. We also study the evolution of the line shapes of the Raman bands due to the longitudinal-optical (LO) phonons. Asymmetries and broadenings of the line shapes are detected. They follow patterns similar to those

established in other alloy semiconductors. We establish that the behavior of the Raman line shapes can be correlated with the magnitude of the frequency splitting between the longitudinal and transverse modes. Our findings constitute a test ground for the models that try to explain the asymmetrical broadenings by invoking specific microscopic interactions in the alloy system. We find that the calculated line shapes with the discrete-continuum interaction model<sup>7,8</sup> reproduce the measured spectra more satisfactorily than the predicted curves evaluated with the spatial-correlation model.<sup>9</sup>

The  $\text{Cd}_{1-x}\text{Zn}_x\text{Te}$  layers with typical thickness of 1 to 3  $\mu\text{m}$  were grown by MBE on GaAs (001) substrates. The Zn content was determined by energy-dispersive analysis of x-rays (EDAX). For  $x \geq 0.1$  the crystalline orientation of the layers is (001) and for  $x < 0.1$  is (111). For the Raman scattering measurements, the samples were mounted in a cold finger of a closed-cycle cryostat and the sample temperature was kept at  $\approx 12$  K. The 6471- and 6764-Å lines of a Kr-ion laser and several lines of a Rhodamine 6G dye-laser excited the Raman spectra. The energy of the incoming photons was tuned to 100 to 200 meV above the fundamental gaps of the samples,<sup>3</sup> in order to obtain through the resonant enhancement a good signal-to-noise ratio. The scattered light was analyzed with a Spex double monochromator and was detected with a GaAs photomultiplier equipped with photon-counting electronics. The backscattering geometry was used with incoming and outgoing polarizations of the photons along the (110) directions. The selection rules for the zinc-blende structure allow scattering by transverse-optical (TO) and longitudinal-optical (LO) phonons in the case of the (111) surfaces and only by LO-like modes in the case of (001) surfaces. Some TO intensity appears in the spectra taken from (001) surfaces in part because of the large angle of

incidence, which was close to the Brewster angle.

Typical first-order Raman spectra of the samples investigated are displayed in Fig. 1. For the ternary samples the spectra consist of four Raman bands. These can be classified in two main groups. One of the groups involves the Raman lines labeled  $LO_1$  and  $TO_1$ . These lines have the character of the LO and TO vibrations of ZnTe ( $x=1$ ). The other group is made of the  $LO_2$  and  $TO_2$  Raman peaks which originate in CdTe ( $x=0$ )-like phonons. In the spectra of Fig. 1 the  $LO_1$  peaks dominate in intensity. The presence of the four Raman lines for intermediate values of  $x$  is typical of a two-mode system. This kind of behavior, which was earlier established for  $Cd_{1-x}Zn_xTe$ ,<sup>5,6</sup> becomes more evident with the information of Fig. 2. In this figure, the frequencies of the modes grouped as explained before are plotted as a function of the Zn content. The solid lines are interpolations through the experimental points as visual aids and the dashed lines represent the extrapolations of the lattice frequencies to the local-mode frequency of Zn in CdTe and to the gap-mode frequency of Cd in ZnTe. The overall behavior of the frequencies as a function of  $x$  is similar to that reported for other two-mode alloys.<sup>10</sup> The measured frequencies of the TO and LO phonons of the CdTe and ZnTe layers are in agreement within the experimental uncertainties ( $\pm 0.2 \text{ cm}^{-1}$ ) with the values measured in bulk samples. The extrapolations made in Fig. 2 predict a value of  $174 \text{ cm}^{-1}$  for the local-mode frequency of Zn in CdTe and  $145 \text{ cm}^{-1}$  for the gap mode of Cd in ZnTe. These numbers compare very favorably with the published values for such frequencies of 167 and  $153 \text{ cm}^{-1}$ , respectively, which were determined at room temperature from reflectivity measurements.<sup>10</sup> The different values of the local-mode frequency can be attributed to the effect of the temperature. For the gap-mode frequency, we cannot invoke

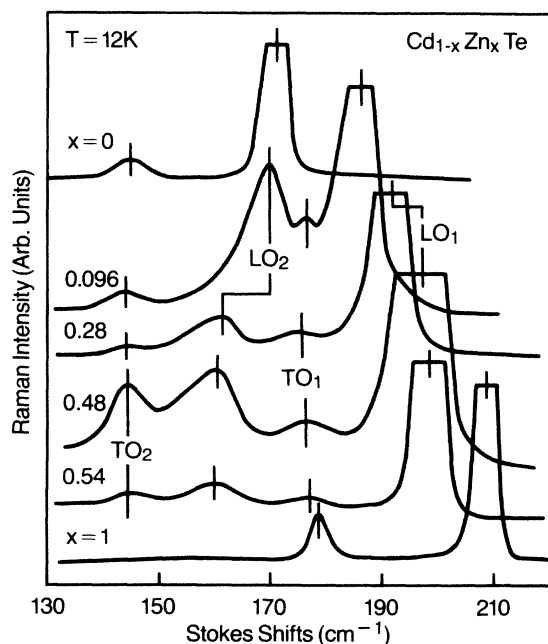


FIG. 1. First-order Raman spectra of  $Cd_{1-x}Zn_xTe$  for various values of  $x$ .

frequency shift due to temperature to explain the difference. We note that the Raman frequencies of the local and gap modes are closer (within  $\approx 10\%$ ) than the reflectivity determined ones to the values of such modes calculated with the assumption of mass substitution.<sup>10</sup>

The results presented in Figs. 1 and 2 confirm the characteristics of the lattice dynamic of  $Cd_{1-x}Zn_xTe$  in terms of being a two-mode system. The major quantitative difference between our measurements and those reported in Refs. 5 and 6 is that we obtained a weaker dependence of the  $TO_2$  frequency as a function of the Zn content. On the basis of the observed two-mode behavior, an effective dielectric function with contributions from two oscillators can be written

$$\epsilon(\omega) = \epsilon_{\infty} + \sum_{i=1,2} S_i \omega_{TO}^2(i) / [\omega_{TO}^2(i) - \omega^2], \quad (1)$$

where  $\epsilon_{\infty}$  is the high-frequency dielectric constant and  $S_i$  is the mode oscillator strength. The zeros of Eq. (1) are at the frequencies of the LO modes  $\omega_{LO}(i)$ . From the measured values of  $\omega_{TO}(i)$  and  $\omega_{LO}(i)$  and by solving  $\epsilon(\omega)=0$  with  $\epsilon_{\infty}=7.5$ , we obtain for  $S_i$  the values quoted in Table I. The values of  $S_1$  and  $S_2$  are approximate due to the uncertainties in  $\omega(i)$  and  $\epsilon_{\infty}$ . Nevertheless, they should be useful in evaluating the effect of phonon scattering on the transport properties.

A related aspect of the Raman investigation of the lattice dynamic of alloy system is the behavior of the Raman line shapes as a function of the composition. In the case of III-V semiconductor alloys, asymmetrical broadenings of the Raman bands have been measured.<sup>7,9,11,12</sup> However, the theoretical explanations of such asymmetries in terms of the microscopic mechanisms that produce them are somehow controversial.<sup>7,9</sup> In what follows, we will consider in detail the evolutions of the  $LO_1$  and  $LO_2$  line shapes of  $Cd_{1-x}Zn_xTe$  as a function of  $x$ . We will also compare our results with published data for III-V alloys and with the predictions of the theoretical models.

The  $LO_1$  and  $LO_2$  bands of Fig. 1 are singled out and plotted in a window of  $-10$  to  $10 \text{ cm}^{-1}$  around their peaks in Fig. 3. The  $LO_1$  lines show a symmetrical profile

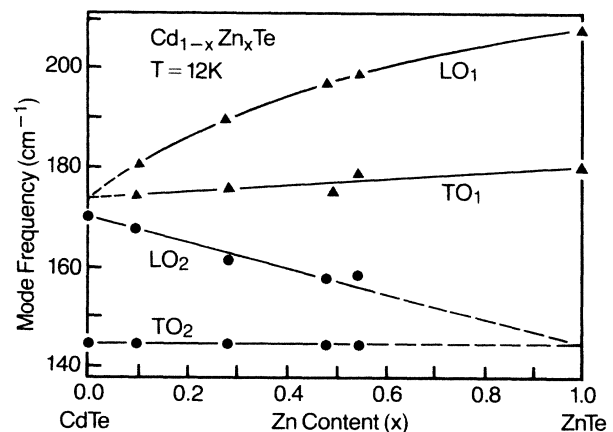


FIG. 2. Compositional dependence of the Raman peak frequencies observed in Fig. 1. The solid lines are drawn as visual aids. The dashed lines represent extrapolated values of the frequencies for the binary limits.

TABLE I. Summary of parameters obtained for the measured  $\text{Cd}_{1-x}\text{Zn}_x\text{Te}$  samples.  $S_1$  and  $S_2$  are the mode oscillator strengths determined with Eq. (1).  $Q$  and  $\Gamma$  are the asymmetry parameter and broadening of the Fano line shape given by Eq. (2), respectively.

Sample	$x$	$S_1$	$S_2$	$Q$		$\Gamma$ ( $\text{cm}^{-1}$ )	
				$\text{LO}_1$	$\text{LO}_2$	$\text{LO}_1$	$\text{LO}_2$
1	0		2.95				1.5
2	0.096	0.149	3.3	-6	40	5.4	8
3	0.28	0.59	2.72	-20	-20	4.6	10
4	0.48	1.1	2.74	-40	-3	6	10
5	0.54	1.02	2.54	-100	-2.5	5	14
6	1	2.62					1.5

for  $x=0.54$ ,  $0.48$ , and  $0.28$ . Their linewidths are  $\sim 5 \text{ cm}^{-1}$  larger than that of the LO mode of ZnTe. For  $x=0.096$ , the line shape develops an asymmetry to the low-energy side. On the other hand, the CdTe-like  $\text{LO}_2$  modes show an increasingly large asymmetrical broadening with increasing concentration. One way in which the observed asymmetries can be quantified is by taking the ratio of the linewidths measured at half maximum to the left and to the right of the peak frequency (as in Ref. 9). With this empirical procedure, we obtain the dependence of the asymmetry of the LO modes of  $\text{Cd}_{1-x}\text{Zn}_x\text{Te}$  which is shown in Fig. 4. Similar data for the  $\text{Ga}_{1-x}\text{Al}_x\text{As}$  system inferred from Fig. 3 of Ref. 9 are also plotted in this figure. The  $\text{LO}_1$  mode of  $\text{Ga}_{1-x}\text{Al}_x\text{As}$  corresponds to the AlAs-like vibrations and  $\text{LO}_2$  refers to the GaAs-like ones. We compare  $\text{Cd}_{1-x}\text{Zn}_x\text{Te}$  with  $\text{Ga}_{1-x}\text{Al}_x\text{As}$  because the latter is a very well studied system and can be taken as a typical representative of alloy semiconductors. A remarkable similar qualitative behavior of the asymmetry is observed as a function of composition for both systems. Another important observation is that the asymmetry and the broadening of a given LO-like mode increases with decreasing LO-TO splitting for that particular mode, as shown below. These effects, which are pronounced for the  $\text{LO}_2$  modes because the splittings are smaller to begin with, are depicted in Fig. 5. The phonon

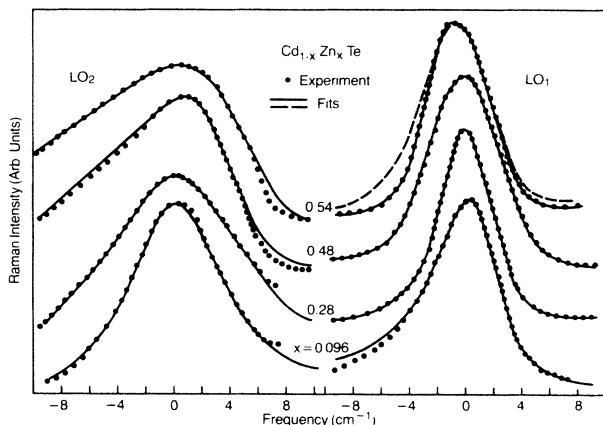


FIG. 3. Measured and calculated line shapes of the LO-like modes of  $\text{Cd}_{1-x}\text{Zn}_x\text{Te}$ .

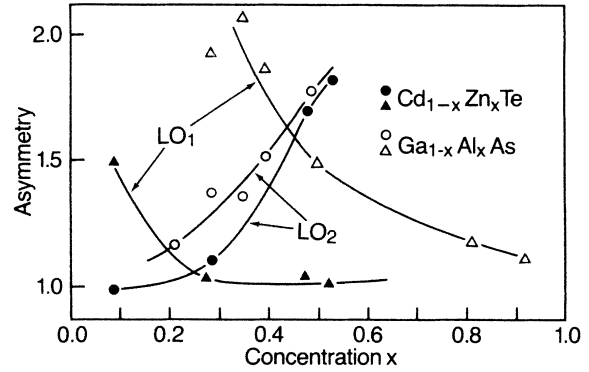


FIG. 4. Concentration dependence of the asymmetry of the LO-like Raman line shapes. The data of  $\text{Ga}_{1-x}\text{Al}_x\text{As}$  were taken from Ref. 9. The lines are drawn as visual aids.

splittings of  $\text{Ga}_{1-x}\text{Al}_x\text{As}$  were taken from Fig. 139 of Ref. 10.

The compilation of data presented in Figs. 4 and 5 strongly suggests that the asymmetrical broadenings of the LO lines are due to a Fano-like effect produced by an anharmonic decay of the LO phonons into a continuum of other phonons.<sup>7</sup> The discrete-continuum interaction produces the Fano profile for the Raman intensity  $I(\omega)$ , which is given by<sup>7,8</sup>

$$I(\omega) \propto |Q + \eta|^2 / (1 + \eta^2). \quad (2)$$

In this equation  $\eta$  represents the reduced frequency  $(\omega - \omega_0)/\Gamma$  where  $\Gamma$  is the broadening and  $Q$  is the asymmetry parameter. The solid lines in Fig. 3 give the predicted Raman bands with Eq. (2). The values of  $\Gamma$  and  $Q$  that allow the best fits to the experimental lines are tabulated in Table I. The agreement between the theory and the experiment is good. Both, the symmetrical line shapes of the  $\text{LO}_1$  modes (large  $|Q|$ ) and the highly asymmetrical  $\text{LO}_2$  bands (small  $|Q|$ ) are well accounted for. In the framework of the “discrete-continuum interaction” model for the asymmetries to take place, the continuum has to become Raman active. This can be accomplished by disorder-induced scattering due to alloying (see, for in-

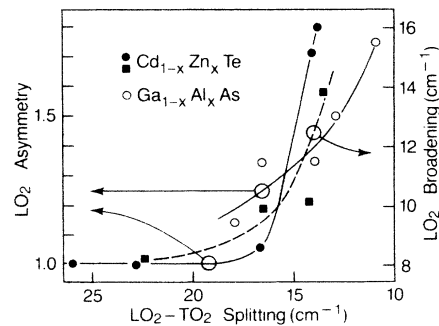


FIG. 5. Broadening and asymmetry of the  $\text{LO}_2$  Raman bands plotted against the corresponding LO-TO splitting. The points for  $\text{Ga}_{1-x}\text{Al}_x\text{As}$  come from the data of Refs. 9 and 10. The solid and dashed lines are drawn as visual aids.

stance, Ref. 13). The elucidation of the exact nature of the possible continuum of interacting phonons has not been attempted in this work. However, we mention two sources which are likely to provide such continuum. One is given by the longitudinal-acoustical phonons. They are expected to overlap in frequency particularly with the LO<sub>2</sub> modes as the Zn content increases.<sup>14,15</sup> The other is the interaction between the LO- and the TO-like modes, in a fashion similar to the relaxation response described by the central peak theory (see, for instance, Ref. 16). Changes in the character of TO modes that behave as LO modes have been reported for heavily doped semiconductors and similar effects can be anticipated for ternary compounds because of the alloy disorder.<sup>17</sup> The patterns depicted in Fig. 5 correlate strongly with this second alternative.

We also evaluated the line shapes using the expression for  $I(\omega)$  proposed in the spatial-correlation model,<sup>9</sup>

$$I(\omega) \propto \int_0^1 \frac{e^{-q^2 L^2/4}}{[\omega - \omega(q)]^2 + (\Gamma_0/2)^2} d^3q. \quad (3)$$

In Eq. (3)  $\Gamma_0$  is the width of the LO lines of the end point materials ( $\approx 1.5 \text{ cm}^{-1}$ ),  $L$  is the correlation length and serves as the fitting parameter, and  $\omega(q)$  represents the LO phonon dispersion which is taken to be given by

$$\omega^2(q) = A + [A^2 - B(1 - \cos\pi q)]^{1/2}. \quad (4)$$

From the measured dispersion curves with neutron scattering,<sup>14,15</sup> we determined for CdTe  $A = 1.445 \times 10^4 \text{ cm}^{-2}$  and  $B = 9.88 \times 10^7 \text{ cm}^{-4}$ , and for ZnTe,

$A = 2.1632 \times 10^4 \text{ cm}^{-2}$  and  $B = 1.637 \times 10^8 \text{ cm}^{-4}$ . The calculated line shapes with Eqs. (3) and (4) reproduce the LO<sub>2</sub>-measured ones in a similar fashion as the solid lines of Fig. 3. We obtained values for  $L$  of 15, 10, 9, and 8 Å for  $x = 0.096, 0.28, 0.48,$  and  $0.54$ , respectively. However, when we tried to fit the LO<sub>1</sub> line shapes, in order to reproduce the measured widths for  $x = 0.48$  and  $0.54$ , the theory imposes the low-energy tail shown by the dashed line of Fig. 3. This tail gives an asymmetry not observed experimentally and, therefore, we conclude that the spatial-correlation model does not reproduce the measured line shapes for all values of  $x$ . A similar conclusion has been recently reached in the case of GaAs<sub>1-x</sub>Sb<sub>x</sub>.<sup>12</sup>

In summary, we have performed a Raman scattering investigation of the lattice dynamic properties of layers of Cd<sub>1-x</sub>Zn<sub>x</sub>Te. We have investigated the compositional dependence of the frequencies of the long-wavelength phonons and their Raman line shapes. An empirical correlation has been established between the behaviors of the line-shapes parameters and the magnitude of the LO-TO splittings. Such a correlation, which appears to be a general characteristic of two-mode alloy semiconductors, provides supportive experimental evidence for the discrete-continuum interaction model.

We would like to acknowledge K. Kiss for the help with the EDAX measurements. The work at the University of Illinois at Chicago has been supported by the Defense Advanced Research Projects Administration under Contract No. MDA 903-83K-0251.

<sup>1</sup>See, for example, the Proceedings of the U.S. Workshop on the Physics and Chemistry of Mercury Cadmium Telluride (MCT) [J. Vac. Sci. Technol. 21, No. 1 (1982)]; A 1, No. 3 (1983); A 3, No. 1 (1985).

<sup>2</sup>J. H. Dinan and S. B. Qadri, J. Vac. Sci. Technol. A 3, 851 (1985).

<sup>3</sup>D. J. Olego, J. P. Faurie, S. Sivanathan, and P. M. Raccah, Appl. Phys. Lett. 47, 1172 (1985).

<sup>4</sup>N. Motta, A. Balzarotti, P. Letardi, A. Kisiel, M. Czyzyk, M. Zimnal, and M. Podgorny, Solid State Commun. 53, 509 (1985).

<sup>5</sup>H. Harada and S. Narita, J. Phys. Soc. Jpn. 30, 1628 (1971).

<sup>6</sup>L. K. Vodopyanov, E. A. Vinogradov, A. M. Blinov, and V. A. Rukavishnikov, Fiz. Tverd. Tela (Leningrad) 14, 268 (1972) [Sov. Phys.—Solid State 14, 219 (1972)].

<sup>7</sup>K. P. Jain and M. Balkanski, in *Light Scattering in Solids*, edited by M. Balkanski, R. C. C. Leite, and S. P. S. Porto (Flammarion, Paris, 1976), p. 106.

<sup>8</sup>G. Abstreiter, M. Cardona, and A. Pinczuk, in *Light Scattering in Solids IV*, edited by M. Cardona and G. Güntherodt

(Springer, Heidelberg, 1984), p. 5.

<sup>9</sup>P. Parayanthal and F. H. Pollak, Phys. Rev. Lett. 52, 1822 (1984).

<sup>10</sup>A. S. Barker and A. J. Sievers, Rev. Mod. Phys. 47, S1 (1975), and references therein.

<sup>11</sup>R. Beserman, C. Hirlimann, M. Balkanski, and J. Chevallier, Solid State Commun. 20, 485 (1976).

<sup>12</sup>R. M. Cohen, M. J. Cherng, R. E. Brenner, and G. B. Stringfellow, J. Appl. Phys. 57, 4817 (1985).

<sup>13</sup>M. Cardona, in *Light Scattering in Solids II*, edited by M. Cardona and G. Güntherodt (Springer, Heidelberg, 1982), p. 19, and references therein.

<sup>14</sup>J. M. Rowe, R. M. Nicklow, D. L. Price, and K. Zanio, Phys. Rev. B 10, 671 (1974).

<sup>15</sup>N. Vegelatos, D. Wehne, and J. S. King, J. Chem. Phys. 60, 3613 (1974).

<sup>16</sup>W. Hayes and R. Loudon, in *Scattering of Light by Crystals* (Wiley, New York, 1978), and references therein.

<sup>17</sup>D. J. Olego and M. Cardona, Phys. Rev. B 24, 7217 (1981).